ESR centers, interface states, and oxide fixed charge in thermally oxidized silicon wafers

Philip J. Caplan, Edward H. Poindexter, Bruce E. Deal, and Reda R. Razouk

Citation: Journal of Applied Physics **50**, 5847 (1979); doi: 10.1063/1.326732
View online: http://dx.doi.org/10.1063/1.326732
View Table of Contents: http://scitation.aip.org/content/aip/journal/jap/50/9?ver=pdfcov
Published by the AIP Publishing

ESR centers, interface states, and oxide fixed charge in thermally oxidized silicon wafers

Philip J. Caplan and Edward H. Poindexter
U.S. Army Electronics Technology and Devices Laboratory, Fort Monmouth, New Jersey 07703

Bruce E. Deal and Reda R. Razouk
Research and Development Laboratory, Fairchild Camera and Instrument Corporation, Palo Alto, California 94304

(Received 5 March 1979; accepted for publication 15 May 1979)

The ESR P_b center has been observed in thermally oxidized single-crystal silicon wafers, and compared with oxide fixed charge Q_{ss} and oxidation-induced interface states N_{st}. The P_b center is found to be located near the interface on (111) wafers. Its g anisotropy is very similar to that of known bulk silicon defects having Si^{III} bonded to three other Si atoms; the P_b unpaired electron orbital, however, is exclusively oriented normal to the (111) surface. The P_b center cannot be identified with any other known defect in Si or SiO_2; in particular, it is totally unlike the common E' center of SiO_2. In contrast to Q_{ss}, both P_b and N_{st} were found to be greatly reduced by steam oxidation and hydrogen annealing. Both P_b and N_{st} may be regenerated by subsequent N_2 anneals at 500°C. In a graded series of samples, P_b and N_{st} are found to be proportional and nearly equal in concentration. This possible confirmation of Si^{III} at the interface, and correlation with N_{st}, support the theoretical indication of an Si^{III} band-gap energy level. The E' center is unobservable, and if present, exists only in a concentration well below that of Q_{ss}. Thus, in addition to a lack of strong correlation with P_b, Q_{ss} is evidently not due to E' centers in their normal charge state. Overall, ESR is judged to be a useful technique for research on silicon wafer defects.

PACS numbers: 73.40.Qv, 73.20.Hb, 76.30.Mi

INTRODUCTION

A definitive picture of the silicon/silicon dioxide interface and its associated electrical defect centers continues to be an important goal of device research.[1] Electron spin resonance (ESR) is perhaps the only spectroscopic tool which responds exclusively to defect atomic states in Si/SiO_2 (a perfect system *a priori* gives no signal). Review of early ESR studies,[2-6] together with recent improvements in ESR sensitivity, promoted this present study. Our objectives are to assess the significance of ESR as an analytical tool for the Si/SiO_2 system, and (hopefully) to exploit ESR for clarification of the atomic origins of interface states and oxide fixed charge.

In an early study of oxidized silicon wafers, Nishi[2] found three ESR centers, and subsequently[3] determined their spectroscopic g factors to be 2.000 (isotropic), 2.000–2.010 (anisotropic), and 2.065 (nearly isotropic). He designated them as P_a, P_b, and P_c, respectively, and examined certain aspects of their behavior after different wafer-processing treatments. In other studies, unspecified centers with g values like P_a[4] and P_b[5] were confirmed. The P_c signal was later shown to be due to neutral elemental iron.[6] In none of these studies was there an extensive search for possible correlation of ESR centers with oxide fixed charge Q_{ss} or interface states N_{st}.

Several important areas for extension and improvement in approach are suggested by the early findings, and these are addressed in this present study. First, our wafer samples were prepared with state-of-the-art industrial controls, to reduce confusion and disagreement arising from the great sensitivity of both ESR and interface charge defect centers to subtle variations in processing. Second, we have made liberal use of the vast literature on ESR studies of defects in bulk Si and SiO_2 to deduce a more definitive atomic identification of observed centers. Finally, a substantial number of parallel observations of both ESR defects and interface charge centers were made on wafers processed by a variety of device-relevant procedures. In this way it was hoped to determine any significant correlations and possibly causal relations between paramagnetic and electrical defects.

Of all the ESR signals reported in Si/SiO_2 system, P_b appears to be most pertinent to the inherent defect structure of the interface, whereas P_c is clearly due to iron contamination, and P_a resembles the signal from donor or conduction electrons.[7] This study is mainly concerned with observations of P_b, with some attention to the well-known E' center of damaged SiO_2, together with Q_{ss} and N_{st}.

EXPERIMENTAL PROCEDURES

Wafer Samples

The silicon used for the electrical and oxide thickness measurements was obtained from Fairchild in the form of 2-in.-diam wafers, chem-mechanically polished on one side. Orientations were (111) and (100), and resistivity was 4–6 Ω cm for n-type phosphorus doped (1×10^{15} cm^{-3}), and 5–9 Ω cm for p-type boron doped (1×10^{15} cm^{-3}). Samples for ESR measurements were in the form of 4×20 mm wafer bars, laser or diamond scribed from 2-in.-diam wafers obtained from Monsanto. They were 200–250 μm thick and chem-mechanically polished on both sides. Both n-type phosphorus-doped and p-type boron-doped wafers of resis-

 0021-8979/79/095847-08$01.10

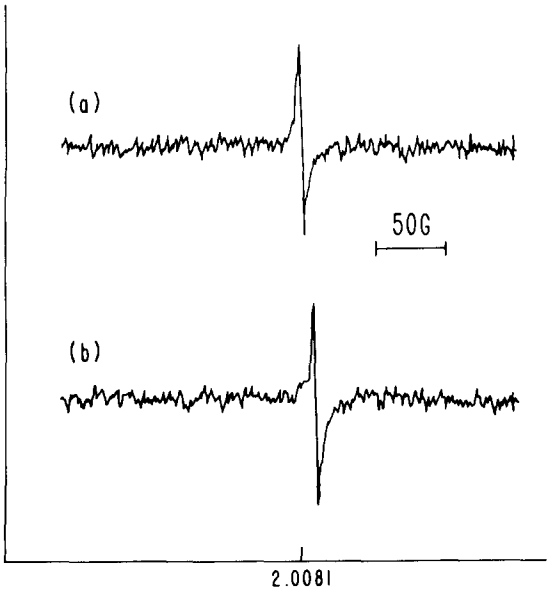

FIG. 1. Single-sweep P_b signal from oxidized (111) silicon wafers. (a) H_0 parallel (111) face; (b) H_0 perpendicular (111) face.

tivity $\geqslant 100\ \Omega$ cm were used. Crystal growth was by the float-zone process with a slice alignment of $\pm$ 1° from (100) or (111), except for p-type (111) wafers, which were 4.0° $\pm$ 0.5° off (111) towards the (110) parallel to the flat.

The cleaning procedure used consisted of the following steps: (a) sulfuric peroxide or hot sulfuric acid (5 min), (b) DI rinse, (c) aqua regia (5 min), (d) DI rinse, (e) water : hydrofluoric acid 10 : 1 (10 sec), (f) DI rinse, (g) isopropanol vapor (3 min). They were then loaded into an oxidation furnace in the appropriate ambient, oxidized for a given time, and then pulled from the furnace in either the oxidizing ambient or in nitrogen. Pull rates varied from 1–3 sec to 10 min. Nitrogen pulls were always preceded by a 10-min-nitrogen purge for dry-O_2 oxidations, and a 15-min purge for H_2O and O_2/HCl oxidations. The oxidation time was chosen to provide oxide thicknesses close to 2000 Å, except for oxidations at 800 °C, where lower thickness values were obtained due to time limitations. Some of the oxides prepared for ESR measurements were annealed in 10% H_2 in N_2 at 500 °C for 10 min.

Dry oxygen was supplied from a liquid source, as were the nitrogen and hydrogen annealing gases. The water oxidation ambient was generated by the direct reaction of H_2 and O_2 in a pyrogenic system. For the HCl/O_2 oxidations, HCl of 99.99% purity was supplied from a gaseous bottle source. Calibrated flowmeters were used to monitor and control gas mixtures in the proper ratios. The oxidation systems were conventional hot-wall resistance-heated furnaces with quartz tubes and high-purity mullite liners. Specially designed boats and holders were used to support the silicon bars during the oxidation and cleaning processes.

After oxidation, aluminum dots (99.999% Al) approximately 1 μm thick and 750 μm in diameter were vacuum deposited at 25 °C on the samples to be measured electrically. To avoid radiation effects, a non-electron-beam flash evaporation system was employed. Oxide thicknesses were determined using a Rudolph Model 436-200E ellipsometer.

ESR Techniques

Spectra (X band) were run initially on a Varian 4501 spectrometer, and afterward on an E-line Century with 9-in. magnet. The ESR observation of the P_b signal was done at room temperature at a nonsaturating power level. Spin concentrations and g values were calculated by comparison with ordinary standards such as weak pitch and Mn in MgO. Generally five wafer bars comprised each sample. Nishi's experiments[3] were done at 77 °K, but once it was established that signals were detectable at room temperature, it became evident that this would be a better method for routine evaluation of a large group of samples. A particular disadvantage of liquid-nitrogen temperature is that the silicon conductivity, and hence cavity losses, are maximum in this temperature range. Temperatures down to near liquid helium were tried with a Helitran cryogenic system, but the gain in overall sensitivity was at best not impressive. Evidently other factors, such as a possible decrease of occupancy of the paramagnetic levels due to temperature shifts of the Fermi level, and saturation occurring at lower power levels, counteract the enhanced detectability of the P_b signal due to the Boltzmann factor.

The single-trace signal-to-noise ratio on oxidized non-hydrogen-annealed (111) wafers ranged up to 40 : 1. For (100) wafers, or for hydogen-annealed samples, the signals were often undetectable on single traces. In these cases a multichannel signal averager was used. In principle such a technique can provide sensitivity limited only by patience and instrumental stability. This would allow observation of ESR signals present at concentrations comparable to state-of-the-art N_{st} values for accumulation of signal over a couple of days. In practice, background signals (not noise) from silicon metallic impurities, sample holders, and perhaps atmospheric oxygen obscure results before this limit is reached. Bulk impurities in silicon at a concentration of one part in 10^9 can mask weak interface signals.

Measurements of oxide fixed charge and interface states

One half of each wafer was annealed in a 10% H_2 in N_2 mixture for 10 min at 500 °C. These postmetallization annealed samples were used for measurement of Q_{ss}, the oxide fixed charge. Conventional C-V analysis equipment was used for this measurement.

Values of N_{st}, the interface–state density, were determined by the quasistaic C-V technique.[8,9] This method is based on the proportionality that exists between the incremental MOS capacitance and the charging current in the structure when it is subjected to a linear voltage ramp. As a result of this proportionality, a low-frequency thermal-equilibrium MOS capacitance-voltage curve can be obtained. The quasistatic and high-frequency curves are then used to extract the interface-state density distribution in the band gap. The method is valid in the interval from the forbidden gap extending from the inversion threshold to a position about 200 mV from the majority-carrier band edge. The relationship between the silicon surface potential and the applied voltage is obtained by the integration of the quasistatic C-V curve.

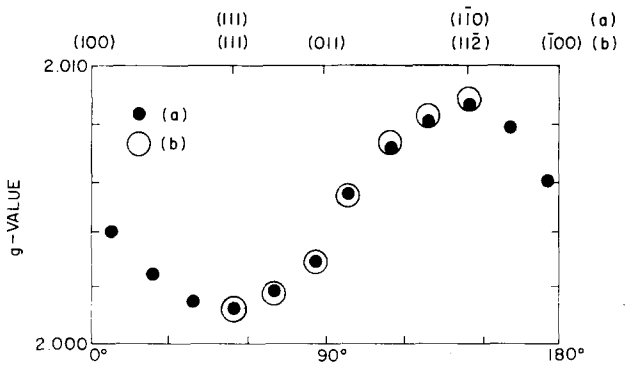

FIG. 2. Anisotropy of g factor for P_b signal on (111) wafers. Rotation plane (a) (11$\bar{2}$); (b) (1$\bar{1}$0).

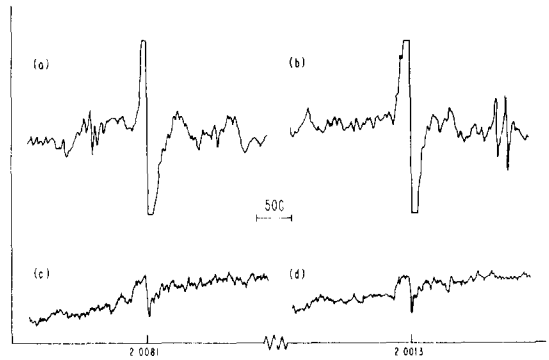

FIG. 3. Multiple-sweep averaged P_b signal from oxidized (111) silicon wafers. (a) H_0 parallel (111) face; (b) H_0 perpendicular (111) face; (c) and (d) corresponding empty sample holder signals. All signals were averaged over 400 sweeps at gain 10 times that of Fig. 1.

Automated measurements of the ramp voltage in conjunction with either the capacitance or the charging current in the MOS structure were used to generate the high-frequency and quasistatic C-V curves, respectively. Accuracy of the quasistatic method in determining interface states is estimated to be 10^{10}/cm^2 eV at midgap.[9] For unannealed samples with high interface-state densities (10^{12}/cm^2 eV), errors in the determination of the energy are high, and at times only the minimum interface-state density can be obtained accurately. In some cases the interface-state density showed a peak or peaks at certain energies, which might well be important in a more detailed study. In the present work, however, only midgap values are reported.

RESULTS AND DISCUSSION

ESR centers on (111) wafers

The essential spectroscopic parameters of the P_b signal (except for signal amplitude) were found not to change meaningfully, regardless of wafer treatment; for detailed spectrum examination, samples showing good signal-to-noise ratio were selected without regard to processing conditions. Specimens oriented with (1$\bar{1}$0) axes along the long side of the chip were examined. Shown in Fig. 1 are single-sweep signals for two orientations in the magnetic field, (111) face $\|H_0$ and (111) $\perp H_0$. The signals show g-factor anisotropy, varying from $g_\| = 2.0012$ along the (111) axis to $g_\perp = 2.0081$ perpendicular to the (111) axis. The perpendicular component is independent of axis of rotation, indicating axial symmetry, and the g ellipsoid is oblate. The anisotropy is plotted in Fig. 2. Note that only one limb is observed, for $g_\|$ exclusively along the (111) axis normal to the interface.

Hyperfine components have not been identified, although the P_b signal usually shows weak structure on the steep wings of the resonance. These have not been consistently resolvable, and may be artifacts. Search for hyperfine structure was made with a signal averager at spectrometer gain 10 times that of Fig. 1. The enhanced signals are shown in Fig. 3. Much detail is evident, but unfortunately most of it seems to be due to background signals from the silicon; empty sample-holder traces with the same spectrometer gain are also shown in Fig. 3. A review of silicon and silicon dioxide defect literature indicates primary hyperfine lines from Si^{29} are usually present with splittings of 50 –200 Oe.[10,11] No symmetrical satellites in this range are discernible amid the background clutter.

Despite lack of hyperfine lines, however, the g value and its anisotropy are readily matched with one and only one type of defect among the more than 40 which have been analyzed in Si and SiO_2. Defects having oblate g ellipsoid, almost rotationally symmetric, with $g_1 \approx g_\| = 1.999$–2.004 and $g_2 \approx g_3 \approx g_\perp = 2.006$–$2.014$, have all been identified

TABLE I. ESR parameters of P_b and common damage centers in irradiated silicon and SiO_2.

Center symbol	g_1	g_2	g_3	Orientation	Model	Ref.
P_b	2.0012	2.0081	2.0081	$g_1\perp$(111) face ($g_1\|$(111) axis)	$\cdot Si{\equiv}Si_3$ in silicon, unbonded orbital perpendicular to (111) interface	...
				Silicon centers		
G-8	2.0005	2.0112	2.0096	$g_1\|$(111) axes	$\cdot Si{\equiv}Si_3$ at Si vacancy near P	13
G-7	2.0012	2.0135	2.0150	$g_1\|$(111) axes	$\cdot Si{\equiv}Si_3$ at divacancy	10
P-1	2.0023	2.0118	2.0106	$g_1\|$(111) axes	$\cdot Si{\equiv}Si_3$ at pentavacancy	14
G-2	2.0151	2.0028	2.0038	$g_1\|$(011) axes	Si–Si bent bond over vacancy	10
B-1	2.0092	2.0026	2.0033	$g_1\|$(011) axes	Si–Si bent bond, vacancy with O	15
G-1	2.0087	1.9989	1.9989	$g_1\|$(100) axes	Si·Si* bent bond over vacancy	16
				SiO_2 centers		
E'	2.0018	2.0005	2.0003	$g_1\perp O_3$ plane	$O_3{\equiv}Si\cdot$ ...*$Si{\equiv}O_3$ at O vacancy	17
HC_1	2.0026	2.0090	2.0210	uncertain	Si–$O\cdot$, hole on nonbridging O	11

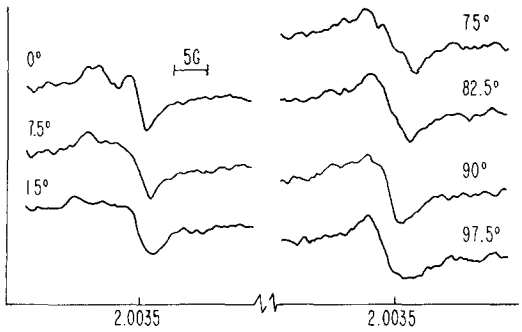

FIG. 4. Multiple-sweep averaged P_b signals from oxidized (100) silicon wafers. H_0 parallel (100) axis at 0°. All signals averaged over 64 sweeps.

with a broken silicon bond on an Si ^{III} atom in silicon, bonded to three other Si atoms, and with unpaired orbital aimed into a vacancy.[10,12–14] Centers comprising one or more Si ^{III} atoms associated with up to five neighboring vacancies have been reported. Other configurations, such as interstitials and reconstructed bent-bond Si–Si defects at Si vacancy/impurity centers,[10,12,15,16] have markedly different g anisotropies. Further, the P_b signal does not resemble in the slightest degree that of the two most common defects in SiO_2: the E' center[11,17,18] and the nonbridging oxygen hole center.[11] The E' center has a prolate g ellipsoid with much smaller anisotropy and has been identified with Si ^{III} unbonded orbital facing into an oxygen vacancy. The g values for common ESR centers are summarized in Table I.

In view of the close resemblance of P_b to the Si ^{III}-vacancy centers, we tentatively identify it with Si ^{III} bonded to three other silicons, with unpaired electron orbital normal to the (111) interface. It will be described structurally as $Si{\equiv}Si_3$ in the following discussion. Etch-back tests caused the P_b center to vanish as the last 50 Å of oxide are removed, and similarly, the P_b concentration is essentially constant above a 50-Å thickness in a graded series of grown oxides.[19] Since it is highly unreasonable to expect preferential broken-bond orientation anywhere in the silicon or silicon dioxide except in the unique region of the interface, the position of the centers is established as being within a monolayer or two of the Si-SiO_2 boundary. That such a high degree of orientational order is indicated by ESR to exist at the interface may or may not be surprising, depending on one's view of the structural violence of the oxidation process.

ESR of (100) wafers

The P_b signal (or more rigorously, the signal with a similar g value) from (100) wafers is much weaker and distinctly different in character from (111) signals. The signal-to-noise ratio is about an order of magnitude worse than (111). Signals for a rotated (100) wafer are shown in Fig. 4. The signal shows a number of poorly defined components. After some primitive deconvolution, the g map shown in Fig. 5 was deduced; but this plot is uncertain at best. It is markedly different from the g map for (111). There are of course no perpendicular unbonded $Si{\equiv}Si_3$ structures expected on (100). For comparison, theoretical g maps for two possible (100) spin centers are also shown. Figure 5(b) represents $Si{\equiv}Si_3$ with unbonded orbital inclined along a (111) axis (G-8 center[13]), and Fig. 5(c) represents a long bent Si–Si bond across a silicon vacancy at the interface (B-1 center[15]). The observed interwoven limbs resemble a superposition of B-1 and inverted G-8 maps. (The isolated invariant limb at 1.997 may be a conduction-electron signal). This unexplained character opens the possibility for partly oxidized centers, such as $Si{\equiv}Si_2O$, which is structurally plausible on the (100) surface. Definition of the (100) P_b center, however, must await better measurements.

Search for E' centers in oxidized silicon

The classic E' center in SiO_2 is a binary structure: an oxygen vacancy with unpaired Si spin on one side, $O_3{\equiv}Si$; and a stripped positively charged $^{+}Si{\equiv}O_3$ on the other side. Because of its common occurrence and its attractivenes as a possible source of oxide fixed charge, we conducted a thorough search for the E' center in some pertinent forms of silica. The spectra are shown in Fig. 6. First, neutron-irradiated quartz powder[20] with many E' centers was tested as a reference, and a strong signal was observed. Second, chemically pure SiO_2 sand was reground in a mortar, and a weaker but unmistakable E' signal was observed. Next, a stack of four oxidized wafers, chosen for high Q_{ss} (6×10^{11} q/cm^2), was run for 2500 repeat traces on the signal averager. Nothing was seen, and comparison with the adjacent P_b reference signal (4×10^{11} spin/cm^2) indicates that the upper limit to E' concentration is 2% of P_b, $\leqslant10^{10}$/cm^2, well below the concentration of oxide fixed charge centers. Finally, in hopes of somehow seeing E' centers in oxidized silicon, a finely pow-

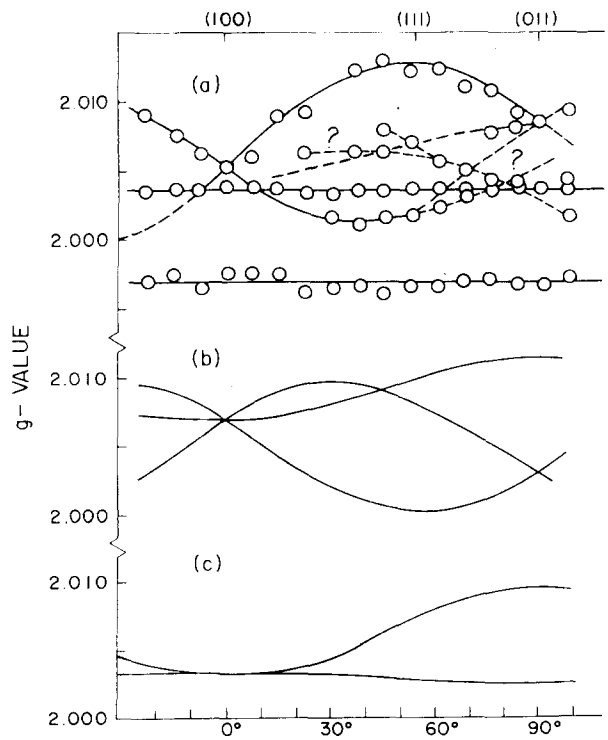

FIG. 5. Anisotropy of g factor for P_b signals on (100) wafers. (a) Observed values; (b) theoretical map for type G-8 $Si{\equiv}Si_3$ center; (c) theoretical map for type B-1 bent-bond orbitals.

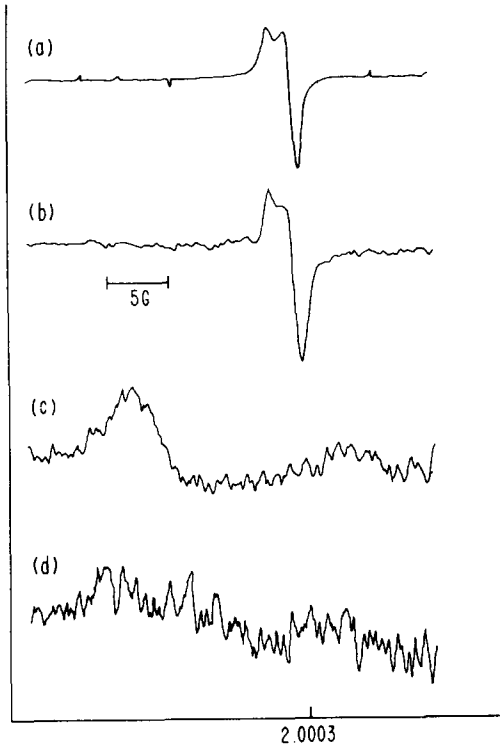

FIG. 6. Search for E' centers in various forms of SiO_2. (a) Neutron-irradiated quartz powder, 1 sweep; (b) recrushed pure silica sand, 150 sweeps; (c) oxidized (111) silicon wafers with high Q_{ss}, 2500 sweeps; (d) oxidized crushed silicon, 2500 sweeps.

dered silicon was oxidized under conditions similar to the wafers, to give an order of magnitude more surface area. At 2500 traces, still no sign of E' signals appeared. We thus conclude that, if present, E' centers must be completely stripped of electrons and in the doubly charged positive state. Alternatively, $^{+}Si{\equiv}O_3$ may be present in the vicinity of the interface in individual sites, rather than in the binary E' structure.

Other possible Si/SiO_2 ESR centers

It might be asked if partially oxidized Si would be expected in the interface—i.e., structures like $^{\cdot}Si{\equiv}Si_2O$ or $^{\cdot}Si{\equiv}SiO_2$.[21] No signals are observed on (111) wafers which can be assigned to such species. The other readily observed signals are P_a and P_c, which have been ascribed to conduction or donor electrons, and iron. The ESR signals expected from partly oxidized Si structures cannot be deduced from any known centers in bulk Si or SiO_2, and it can only be assumed that the g anisotropy would be in some fashion intermediate between $^{\cdot}Si{\equiv}Si_3$ and $^{\cdot}Si{\equiv}O_3$. They would presumably show a triaxial g ellipsoid, and give multilimbed g maps as the wafer is rotated. No such signals are present on (111), and again, if such centers exist there, they are either in low concentration or in the stripped positively charged state, $^{+}Si{\equiv}Si_2O$ or $^{+}Si{\equiv}SiO_2$. Such centers may, however, be pertinent for (100) silicon wafers, as mentioned above.

The various basic (111) site structures containing Si^{III} are shown in Fig. 7. Because of device significance and oft-expressed confusion, both charged and uncharged states are

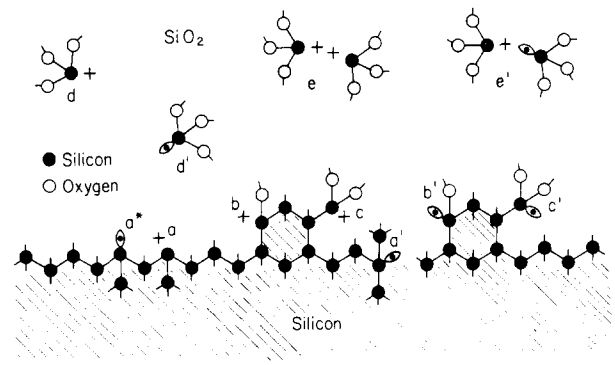

FIG. 7. Basic structural sites containing Si^{III} and situated near Si/SiO_2 interface in oxidized (111) silicon wafers. Detailed explanation in text.

included. (Device researchers typically consider a defect center as one species, regardless of charge state; ESR researchers usually consider each charge state of the center as a distinct species.) It should be noted, however, that charge state is often a function of temperature, voltage, doping level, or proximity to the silicon bulk. The following conclusions on the presence or absence of centers apply to observations at room temperature with no external voltage across the wafer.

Centers labeled a, b, c, d, and e contain no unpaired electron spins, and are *a priori* undetectable by ESR; they might or might not be present. Corresponding centers labeled a', b', c', d', and e' contain an unpaired electron spin, and are presumably detectable. They are not observed, however, and thus can be present in concentrations at most 10^{10} cm^{-2}. The only one of these centers which is clearly present is a^*, i.e., $^{\cdot}Si{\equiv}Si_3$ with an unbonded orbital normal to the interface. The very similar center with other orbital orientations at a' is absent. The partially oxidized silicon centers $^{\cdot}Si{\equiv}Si_2O$ and $^{\cdot}Si{\equiv}SiO_2$ at b' and c' are not observed, but may be present in the states $^{+}Si{\equiv}Si_2O$ and $^{+}Si{\equiv}SiO_2$ at b and

TABLE II. Wafer oxidation and anneal conditions used for comparison of Q_{ss}, N_{st}, and ESR P_b

Ambient/time	Cool/pull conditions
Initial oxidation	
Dry O_2, 800 °C, 4800 min	(a) fast pull in dry O_2 (< 3 sec)
Dry O_2, 1000 °C, 400 min	(b) slow pull in dry O_2 (10 min)
Dry O_2, 1200 °C, 60 min	(c) 10 min purge with N_2, then slow pull in N_2 (2 min)
H_2O, 1000 °C, 18 min	(a) fast pull in steam (< 15 sec) (b) 15 min purge with N_2, then slow pull in N_2 (2 min)
HCl (5%)/O_2, 1000 °C, 215 min HCl (10%)/O_2, 1000 °C, 190 min	(a) 15 min purge with N_2, then slow pull in N_2 (2 min)
Postoxidation anneals	
(1) H_2 (10%)/N_2, 500 °C, 10 min	(a) fast pull in H_2 (10%)/N_2 (< 15 sec)
(2) N_2, 500 °C, 30 min and 120 min (2) N_2, 500 °C, 60 min or 120 min	(b) fast pull in N_2 (< 15 sec)
N_2, 1000 °C, 10 min or 60 min N_2, 1200 °C, 10 min or 60 min	(a) slow pull in N_2 (2 min)
Ar, 1000 °C, 10 min or 60 min Ar, 1200 °C, 10 min or 60 min	(a) slow pull in Ar (2 min)

TABLE III. Concentration of ESR P_b centers as a function of anneals which reduce and the reintroduce interface states.

Oxidation temp (°C)	O_2/N_2 pull times (min)	As-oxidized	P_b concentration (10^{11} spin/cm^2) 500 °C 10 min H_2	500 °C 30 min N_2	500 °C 120 min N_2
1200	60/0/0	3.5	0	1.9	5.4
1200	60/0/2	1.1	0	5.0	4.2
1200	60/10/2	7.3	0	0	1.3
1000	380/0/0	4.7	0	1.5	2.5
1000	360/0/2	5.0	0	0	2.5
1000	360/10/2	11.5	0	2.3	3.7

c. As noted earlier, perhaps they are found on (100). Out in the oxide, $^{+}Si{\equiv}O_3$ at d may be present, but $^{\cdot}Si{\equiv}O_3$ at d′ is absent. These latter two centers might be called hemi-E' centers. The doubly charged pseudo-E' center ($O_3{\equiv}Si^{+}$ ...$^{+}Si{\equiv}O_3$) at e may be present, but the classic binary E' center ($O_3{\equiv}Si^{\cdot}$ ...$^{+}Si{\equiv}O_3$) at e′ is absent from undamaged oxidized wafers.

Not shown in Fig. 7 is the other conceivable charge state of the defect centers, e.g., $^{-}Si{\equiv}Si_3$. As far as ESR is concerned, any of the centers might be present in the negative state. Also missing from Fig. 7 is the other common SiO_2 defect center—the nonbridging oxygen hole center HC_1,[11] which was not observed. Again, this center is either absent, or in an abnormal charge state.

Comparison of ESR centers with oxide fixed charge and interface states

Wafers subjected to a wide variety of processing conditions, summarized in Table II, were used for comparison of the ESR P_b signal with oxide fixed charge and interface states. A comprehensive presentation involving process effects on Q_{ss} and N_{st} for these wafers will be published separately.[22] With respect to the comparison with P_b a number of experimental runs await verification, and accurate quantitative analysis of all data is not completed. Nonetheless, some clear-out features have emerged from this diverse array of about 60 different samples.

(1) P_b, Q_{ss} and N_{st} all initially follow the "oxygen triangle" over the range 800–1200 °C. Inconsistencies noted earlier[19,23] are probably due to inferior controls on oxidation conditions, particularly the critical final cooling atmosphere.

(2) P_b, Q_{ss}, N_{st} are all substantially higher on (111) as compared to (100) wafers.

(3) P_b and N_{st} (but not Q_{ss}) are considerably weaker with steam oxidation.

(4) P_b and N_{st} (but not Q_{ss}) are greatly reduced by hydrogen anneal at 500 °C.

(5) P_b and N_{st} may be regenerated in H_2-annealed wafers by additional extended anneal in N_2 at 500 °C.

Regarding the latter effect, it was already known that reannealing of hydrogen-annealed oxidized silicon, in nitrogen, at temperatures of 500 to 1200 °C, will reintroduce the structural type of interface states.[1] This is probably due to the removal from the oxide of hydrogen which previously complexed the interface states. To determine if P_b centers on (111) silicon could be similarly reintroduced, oxidized p-type bars, first annealed in hydrogen (actually, 10% H_2 in N_2), were reannealed in a nitrogen ambient for 30 min at 500 °C, and subsequently reannealed for 120 min under the latter conditions. The results after each stage are shown in Table III. The oxides were originally oxidized at two temperatures with three different cooling conditions. In all cases it was possible to reintroduce the P_b signal. Some samples showed an even greater P_b signal than originally observed. The reason for this is not clear, although samples processed in nitrogen tend to show higher P_b than those processed in oxygen only.

A parallel N_{st} experiment was carried out using 4–6-Ω-cm (111) silicon wafers, and the results are shown in Fig. 8. The interface-state density distribution for "as oxidized" wafers is shown in curve (a). Curve (b) represents a wafer given a postoxidation hydrogen anneal in a 10% H_2 in N_2 ambient and shows the annealing of interface states. Curves (c) and (d) followed the hydrogen anneal step and a subsequent anneal in nitrogen for 60 and 120 min, respectively, and show the reinducement of interface states. All annealing steps were carried out prior to the deposition of field plates, and a non-electron-beam flash evaporation system was employed in order to avoid radiation effects.

Improved measurements have been obtained on some recent wafer series, which show a good quantitative correlation between P_b and N_{st}. One series comprised n- and p-type wafers oxidized in dry O_2 at 1000 °C and 1200 °C and immediately annealed in N_2 for 10 or 60 min, followed by the usual 2-min N_2 pull. A second series was oxidized in dry O_2 at 1000 °C for times ranging from 2 min to 6 h with fast pull in

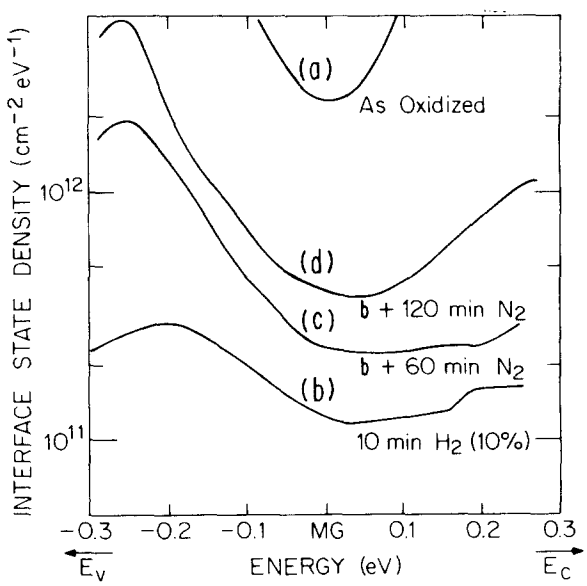

FIG. 8. Interface-state density distributions for n type (111) silicon, oxidized in dry O_2 at 1200 °C, annealed *in situ* in nitrogen for 10 min, and cooled in nitrogen. Distributions shown are for: (a) "as-oxidized wafers"; (b) anneal in 10% H_2 in N_2 at 500 °C for 10 min; (c) anneal as in (b) followed by 60 min in N_2 at 500 °C; (d) anneal as in (b) followed by 120 min in N_2 at 500 °C. All anneals were carried out prior to metallization.

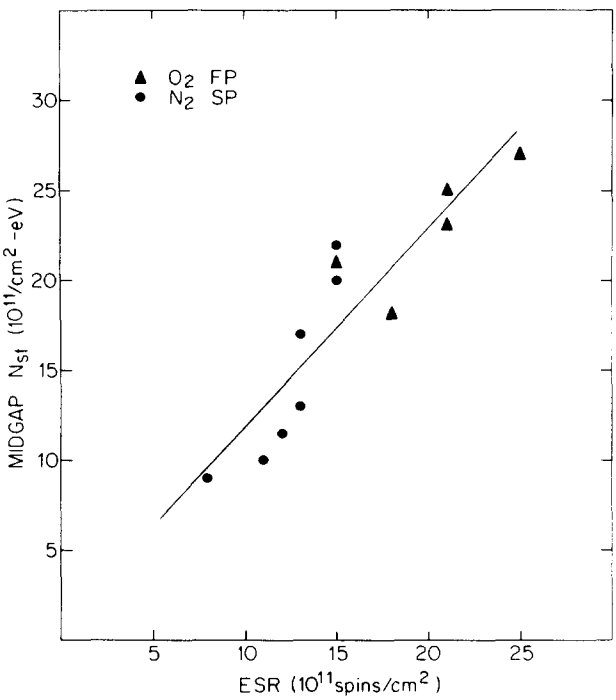

FIG. 9. Midgap interface-state density versus electron spin resonance for n- and p-type (111) silicon, oxidized in dry O_2 and cooled in N_2 or O_2.

O_2 to seek effects of oxide thickness on interface defects. Interface-state density N_{st} and spin concentration of P_b centers for both series are plotted in Fig. 9. The proportionality of N_{st} and P_b is evident, and also of interest is their numerical near equality.

Elaborate interpretation of this plot is not warranted at this time. Samples pulled in oxygen seem to have predominantly donorlike states, while nitrogen-pulled samples show both acceptorlike and donorlike states.[22] Further, the distribution of N_{st} versus energy varies for different processing treatments.[22] So a question arises about the correlation of P_b with the midgap N_{st}; quite possibly, P_b would be better correlated with some other feature of the N_{st} distribution. In this respect, some preliminary evidence indicates that O_2-pulled and N_2-pulled samples may show different N_{st}-vs-P_b slopes. In a different consideration, P_b amplitude reflects not only the concentration, but also the charge condition of a particular species. A zero-biased n-type sample containing acceptorlike states in the lower half of the band gap would exhibit a stronger ESR signal than a similar sample with donorlike states. Despite these reservations, however, the proportionality and numerical equality of N_{st} and P_b are good evidence of a possible causal relation.

In a related study, Nishi *et al.*[24] examined the relation between P_b concentration and surface-electron mobility. In a series of samples with variable steam concentration in the oxidizing ambient, it was found that the ESR signal decreased and the surface mobility increased with increasing partial pressure of water. Since surface-electron mobility is reduced as interface-state density increases, this experiment and ours are mutually consistent. We differ, however, in the interpretation, since Nishi identifies P_b with Q_{ss} on the basis of etch-back profiles, whereas we identify P_b with N_{st}.

In summary, ESR is shown to have considerable merit as an interface characterization tool. The ESR P_b signal on oxidized (111) silicon wafers can be reasonably identified with trivalent silicon, in silicon, bonded to three other silicon atoms, with unpaired spin in nonbonded orbital perpendicular to the interface. Uncharged structures with trivalent silicon bonded to one or more oxygens and fewer silicons are not found on (111) wafers, but may exist on (100) wafers, where the P_b signal anisotropy is not resolvable at this time. The common E' center of damaged SiO_2 is not observed at all, which means that this center in classic form cannot be the main source of the oxide fixed charge Q_{ss}. The P_b center, however, shows a fairly good correlation with N_{st} as measured at midgap on variously processed wafers, but apparently has only an indirect correlation with Q_{ss}, in situations where N_{st} is also correlated with Q_{ss}. The results to date suggest that trivalent silicon may well be a source of a significant fraction of those interface states associated with the thermal oxidation process. This is in accord with old suppositions, and with recent theoretical demonstrations of an $Si{\equiv}Si_3$ near-midgap-energy level[25] and corroborative electrical measurements.[22,26]

ACKNOWLEDGMENTS

The authors would like to thank Julia Bien and Edward Dovichi for conducting various portions of the experimental work, and Dr. J.M. Early for his support and helpful suggestions during the course of this program. A portion of this work has been sponsored by ECOM contract No. DAAB07-77-C-2665 and ARO contract No. DAAG29-78-C-0033.

[1]B.E. Deal, in *Semiconductor Silicon* 1977 (Electrochemical Society, Princeton, N.J., 1977), p. 276.
[2]Y. Nishi, Jpn. J. Appl. Phys. **5**, 333 (1965).
[3]Y. Nishi, Jpn. J. Appl. Phys. **10**, 52 (1971).
[4]A.G. Revesz and B. Goldstein, Surface Sci. **14**, 361 (1969).
[5]I. Shiota, N. Miyamoto, and J.-i. Nishizawa, Surf. Sci. **36**, 414 (1973).
[6]P.J. Caplan, J.N. Helbert, B.E. Wagner, and E.H. Poindexter, Surf. Sci. **54**, 33 (1976).
[7]R.C. Fletcher, W.A. Yager, G.L. Pearson, and F.R. Merritt, Phys. Rev. **95**, 844 (1954).
[8]C.N. Berglund, IEEE Trans. Electron Devices **ED-13**, 701 (1966).
[9]M. Kuhn, Solid-State Electron. **13**, 873 (1970).
[10]J.W. Corbett, *Electron Radiation Damage in Semiconductors and Metals* (Academic, New York, 1966), pp. 60–66.
[11]D.L. Griscom, in *Defects in Non-Metallic Solids* (Plenum, New York, 1976), p. 330.
[12]E.G. Sieverts, Doctoral dissertation, University of Amsterdam, 1978.
[13]G.D. Watkins and J.W. Corbett, Phys. Rev. **134**, A1359 (1964).
[14]Y.-H. Lee and J.W. Corbett, Phys. Rev. B **8**, 2810 (1973).
[15]G.D. Watkins and J.W. Corbett, Phys. Rev. **121**, 1001 (1961).
[16]G.D. Watkins, J. Phys. Soc. Jpn. **18**, Suppl. II, 22 (1963).
[17]F.J. Feigl, W.B. Fowler, and K.L. Yip, Solid State Commun. **14**, 225 (1974).
[18]D.L. Griscom, E.J Freibele, and G.H. Sigel, Jr., Solid State Commun. **15** 479 (1974).
[19]E.H. Poindexter, E.R. Ahlstrom, and P.J. Caplan, in *The Physics of* SiO_2 *and its Interfaces* (Pergamon, New York, 1978), p. 227.
[20]Kindly loaned by Prof. D.L. Cowan, Department of Physics, University of Missouri, Columbia.

[21]V.G. Litovchenko and A.P. Gorban, *Proc. Kiev Science Conference* (Academy of Science, Ukrainian SSR, Kiev, 1978), p. 102.
[22]R.R. Razouk and B.E. Deal, J. Electrochem. Soc. (to be published).
[23]E.H. Poindexter, J.N. Helbert, B.E. Wagner, and P.J. Caplan, IEEE Trans. Electron Devices **ED-24**, 1217 (1977).
[24]Y. Nishi, K. Tanaka, and A. Ohwada, Jpn. J. Appl. Phys. 11, 85 (1972).
[25]R.B. Laughlin, J.D. Joannopoulos, and D.J. Chadi in *The Physics of* SiO_2 *and its Interfaces* (Pergamon, New York, 1978), p. 321.
[26]N.M. Johnson, D.J. Bartelink, and M. Schulz, in *The Physics of* SiO_2 *and its Interfaces* (Pergamon, New York, 1978), p. 421.